Journal of Applied Mechanics and Technical Physics, Vol. 38, No. 1, 1997

SOLUTION OF THE CONTACT PROBLEM FOR A PIN-LOADED PLATE

V. N. Solodovnikov

UDC 539.3.01

We solve the problem of tension of an elastic rectangular plate with a circular hole in which, with a small clearance, an absolutely rigid immovable pin of circular cross section is inserted without friction. The finite-element method is used, and two variants of boundary conditions are imposed on the hole contour Γ.

In one variant, the boundary conditions are formulated for projections of displacements and forces onto the normal and the tangent to Γ. In contrast to [1], the possibility of violation of the condition of impenetration of the hole edge into the pin contour is excluded. The other variant of boundary conditions is obtained by linearizing the impenetration condition. This condition was formulated in [2] in terms of the Cartesian displacement components, but its geometrical sense was not explained. Nor was the form of the boundary conditions adopted for forces presented. In [3], a similar problem was solved for the case of the absence of a gap.

In the algorithm developed below, we assume, as in [2–4], that the contact region occupies one segment of length l on Γ. The region can depend on the load, the gap, and on the adopted variant of boundary conditions. The plate is loaded by the displacement v of its right-hand side. The value of v corresponding to the length l is determined in accordance with the Boussinesq principle [2–6] from the requirement of a zero normal force at the extreme point of the contact region. A solution of the contact problem is sought in this case (differently than in [2–4]) as a sum of solutions of the other two problems that are independent of v and whose coefficients are linear in v.

The finite-element solutions are analyzed. In the first variant, the solution is linear with the gap c, while in the second variant, for each new value of c the problem should be solved again. The form of the solutions is found under unlimited growth of v. The maximum possible length of the contact region $l = l_*$ is determined.

The difference between the solutions calculated for the same displacement v but for different variants of boundary conditions is slight. However, the second variant yields a more precise solution in the sense that it yields a smaller strain energy of the plate, maximum stresses, and length of the contact region. To obtain the same displacement v, one should apply a lesser total tensile force P. In the second variant, with the growth of c the maximum length $l = l_*$ decreases almost as a linear function of c. In the first variant, the length is constant, and its value is the same as in the case of absence of a gap.

1. Basic Equations. Expressions of strains in terms of displacements, relations of Hooke's law, and the equilibrium equations in a plane stressed state in the Cartesian system of coordinates x_1 and x_2 are used in the form [7]

$$e_{11} = u_{1,1}, \quad e_{22} = u_{2,2}, \quad 2e_{12} = u_{1,2} + u_{2,1}, \quad e_{11} = E^{-1}(\sigma_{11} - \nu\sigma_{22}),$$
$$e_{22} = E^{-1}(\sigma_{22} - \nu\sigma_{11}), \quad e_{12} = (1+\nu)E^{-1}\sigma_{12}, \quad \sigma_{11,1} + \sigma_{12,2} = 0, \quad \sigma_{12,1} + \sigma_{22,2} = 0. \tag{1.1}$$

Here E is Young's modulus, ν is Poisson's ratio, u_i are the displacements, e_{ij} are the strains, σ_{ij} are the stresses ($i, j = 1, 2$), and the subscripts 1 and 2 after the commas denote the partial differentiation with respect to x_1 and x_2, respectively.

Lavrent'ev Institute of Hydrodynamics, Siberian Division, Russian Academy of Sciences, Novosibirsk 630090. Translated from Prikladnaya Mekhanika i Tekhnicheskaya Fizika, Vol. 38, No. 1, pp. 121–127, January–February, 1997. Original article submitted March 21, 1995; revision submitted September 26, 1995.

0021-8944/97/3801-0109 $18.00

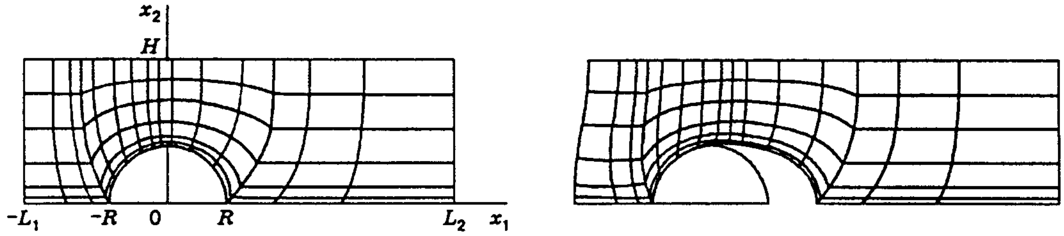

Fig. 1

The strain energy is determined by the formula

$$\Phi = \int_{\Omega} \frac{E}{2(1-\nu^2)} [e_{11}^2 + 2\nu e_{11} e_{22} + e_{22}^2 + 2(1-\nu) e_{12}^2] \, dx_1 dx_2. \tag{1.2}$$

The plate thickness is assumed to be constant and, without loss of generality, to be equal to unity. Integration is performed over the region Ω occupied by the plate.

2. Boundary Conditions. There is a rectangular plate with a noncentral circular hole of radius R. Its half is shown at the left of Fig. 1. The left-hand side of the plate $x_1 = -L_1$ is not loaded, while its right-hand side $x_1 = L_2$ shifts without deformation in the direction of the x_1 axis for $u_1 = v$. Specifying the symmetry conditions for the solution with $x_2 = 0$ and $x_2 = \pm H$, we have

$$\begin{array}{lllll} \sigma_{11} = \sigma_{12} = 0 & \text{for} & x_1 = -L_1, & 0 \leqslant x_2 \leqslant H, & \\ u_1 = v, \ u_2 = 0 & \text{for} & x_1 = L_2, & 0 \leqslant x_2 \leqslant H, & \\ u_2 = 0, \ \sigma_{12} = 0 & \text{for} & x_2 = H, & -L_1 \leqslant x_1 \leqslant L_2 & \text{and} \\ & \text{for} & x_2 = 0, & -L_1 \leqslant x_1 \leqslant -R, & R \leqslant x_1 \leqslant L_2. \end{array} \tag{2.1}$$

An absolutely rigid immovable pin of circular cross section with radius $R_1 = R - c$ and center at a point with Cartesian coordinates $(-c, 0)$ is inserted without friction in the hole with a small clearance ($c = \varepsilon R$, where ε is a small dimensionless parameter and $\varepsilon > 0$). We also use the polar system of coordinates r, φ in which $x_1 = r\cos\varphi$ and $x_2 = r\sin\varphi$. At any point of the hole contour Γ, the relations

$$\cos\theta = \rho^{-1}(\varepsilon + \cos\varphi), \quad \sin\theta = \rho^{-1}\sin\varphi, \quad \rho = (1 + \varepsilon^2 + 2\varepsilon\cos\varphi)^{1/2} \tag{2.2}$$

are satisfied, where θ is the angle between the normal to the pin contour at the point that is the closest to the point under consideration on Γ and the x_1 axis. The projections of the displacement and force vectors onto the normal and the tangent to the pin contour u_ρ, u_θ, q_ρ, and q_θ are expressed in terms of the displacement (u_r and u_φ) and stress (σ_{rr}, $\sigma_{\varphi\varphi}$, and $\sigma_{r\varphi}$) components in the polar coordinate system by the formulas

$$\begin{gathered} u_\rho = u_r\cos\alpha - u_\varphi\sin\alpha, \quad u_\theta = u_r\sin\alpha + u_\varphi\cos\alpha, \\ q_\rho = \sigma_{rr}\cos\alpha - \sigma_{r\varphi}\sin\alpha, \quad q_\theta = \sigma_{rr}\sin\alpha + \sigma_{r\varphi}\cos\alpha, \quad \alpha = \varphi - \theta. \end{gathered} \tag{2.3}$$

The condition of impenetration of the hole edge through the pin contour is represented as

$$\begin{aligned} (R\cos\varphi + c + u_1)^2 + (R\sin\varphi + u_2)^2 &= (\rho\, R + u_\rho)^2 + u_\theta^2 \\ &= (R + c\cos\varphi + u_r)^2 + (u_\varphi - c\sin\varphi)^2 \geqslant R_1^2 = (1-\varepsilon)^2 R^2 \end{aligned} \tag{2.4}$$

or

$$u_\rho + (2\rho R)^{-1}(u_\rho^2 + u_\theta^2) \geqslant u_{\rho c}, \quad u_{\rho c} = -c\rho^{-1}(1 + \cos\varphi). \tag{2.5}$$

Linearizing the left-hand part of the latter inequality, we obtain

$$u_\rho \geqslant u_{\rho c}. \tag{2.6}$$

The absolute value of $u_{\rho c}$ is smaller than the distance from the point under consideration on Γ to the pin contour by a small quantity of the order of c^2. Inequality (2.6) is more rigorous than (2.5). This means that displacements that satisfy (2.6) satisfy (2.5) as well.

In view of the absence of friction, the work of forces for any admissible variations in displacements δu_r and δu_φ or δu_ρ and δu_θ on Γ should be zero:

$$\sigma_{rr}\delta u_r + \sigma_{r\varphi}\delta u_\varphi = q_\rho \delta u_\rho + q_\theta \delta u_\theta = 0. \tag{2.7}$$

In the contact region Γ_1, the displacement is $u_\rho = u_{\rho c}$. The hole edge is pressed against the pin and, therefore, $q_\rho < 0$. For $\delta u_\rho = 0$ and arbitrary δu_θ, from (2.7) it follows that $q_\theta = 0$. On the remaining free part of the hole edge Γ_2, we have $\sigma_{rr} = \sigma_{r\varphi} = 0$ or, which is equivalent, $q_\rho = q_\theta = 0$. We obtain the following boundary conditions on $\Gamma = \Gamma_1 \cup \Gamma_2$:

$$u_\rho = u_{\rho c}, \quad q_\theta = 0, \quad q_\rho < 0 \quad \text{on} \quad \Gamma_1, \qquad q_\rho = q_\theta = 0, \quad u_\rho \geqslant u_{\rho c} \quad \text{on} \quad \Gamma_2. \tag{2.8}$$

The regions Γ_1 and Γ_2 are found from the solution of the problem.

If the expressions for u_ρ, $u_{\rho c}$, q_ρ, and q_θ from (2.3) and (2.5) are substituted into (2.8), then with allowance for (2.2), the radical ρ is excluded from (2.8), and ε is included in the expressions for the coefficients of u_r, u_φ, σ_{rr}, and $\sigma_{r\varphi}$. Therefore, the solution obtained using (2.8) can depend nonlinearly on ε.

We now formulate another variant of boundary conditions on Γ with specification of the projections of displacements and forces onto the normal and the tangent to Γ. Impenetration condition (2.4) is not violated for any value of the hoop displacement u_φ if

$$u_r \geqslant u_{rc}, \quad u_{rc} = -c(1 + \cos\varphi). \tag{2.9}$$

The absolute value of u_{rc} is smaller than the distance along the hole radius from the point under consideration on Γ to the pin contour by a small quantity of the order of c^2. Inequality (2.9) is more rigorous than (2.4).

In the contact region Γ_1, which here can differ from that in (2.8), $u_r = u_{rc}$ and $\sigma_{rr} < 0$. With $\delta u_r = 0$ and arbitrary δu_φ, from (2.7), it follows that $\sigma_{r\varphi} = 0$. On the free part of the hole edge Γ_2, we have $\sigma_{rr} = \sigma_{r\varphi} = 0$. We obtain the boundary conditions

$$u_r = u_{rc}, \quad \sigma_{r\varphi} = 0, \quad \sigma_{rr} < 0 \quad \text{on} \quad \Gamma_1, \qquad \sigma_{rr} = \sigma_{r\varphi} = 0, \quad u_r \geqslant u_{rc} \quad \text{on} \quad \Gamma_2. \tag{2.10}$$

The regions Γ_1 and Γ_2 are determined from the solution of the problem. In this case, the quantities v and c enter the right-hand sides of (2.1) and (2.10) in a linear manner.

Thus, we have two contact problems: (1.1), (2.1), and (2.8) and (1.1), (2.1), and (2.10), each having a unique solution. As a functional of displacements that satisfy the boundary conditions for displacements in (2.1) and the inequality $u_r \geqslant u_{rc}$ or $u_\rho \geqslant u_{\rho c}$ in the case of using (2.8) on Γ, the strain energy Φ reaches a minimum on the solution of problems (1.1), (2.1), and (2.10) and (1.1), (2.1), and (2.8), respectively.

In the absence of a gap ($c = 0$), the following boundary conditions [3] follow from both (2.8) and (2.10):

$$u_r = 0, \quad \sigma_{r\varphi} = 0, \quad \sigma_{rr} < 0 \quad \text{on} \quad \Gamma_1, \qquad \sigma_{rr} = \sigma_{r\varphi} = 0, \quad u_r \geqslant 0 \quad \text{on} \quad \Gamma_2, \tag{2.11}$$

where Γ_1 and Γ_2 are not dependent on the displacement v.

3. Determination of the Contact Region. It is assumed that in any problem the contact region Γ_1 occupies a certain section $0 \leqslant \eta \leqslant l$ ($\eta = 1 - \varphi/\pi$). Its dimensionless length l can depend on the gap c, displacement v, and the adopted variant of boundary conditions (2.8), (2.10), or (2.11).

In the algorithm developed below, the value of l is given. On Γ, we set the boundary conditions obtained from (2.8) or (2.10) by eliminating the restrictions formulated in terms of the inequalities

$$u_r = u_{rc}, \quad \sigma_{r\varphi} = 0 \quad \text{for} \quad 0 \leqslant \eta \leqslant l, \qquad \sigma_{rr} = \sigma_{r\varphi} = 0 \quad \text{for} \quad l < \eta \leqslant 1 \tag{3.1}$$

or

$$u_\rho = u_{\rho c}, \quad q_\theta = 0 \quad \text{for} \quad 0 \leqslant \eta \leqslant l, \qquad q_\rho = q_\theta = 0 \quad \text{for} \quad l < \eta \leqslant 1. \tag{3.2}$$

The equilibrium states of the plate with a given contact region are determined from the solution of problems (1.1), (2.1), and (3.1) and (1.1), (2.1), and (3.2) [called below problems (a) and (b), respectively].

We also define problems ($a1$), ($a2$) and ($b1$), ($b2$). Their only difference from (a) and (b) is that in the boundary conditions for the contact region $0 \leqslant \eta \leqslant l$ we specify $u_r = 0$ in ($a1$), $u_r = c^{-1}u_{rc}$ in ($a2$), $u_\rho = 0$ in ($b1$), and $u_\rho = c^{-1}u_{\rho c}$ in ($b2$), while on the right-hand side of the plate ($x_1 = L_2$ and $0 \leqslant x_2 \leqslant H$) we assume $u_1 = 1$ in ($a1$) and ($b1$) and $u_1 = 0$ in ($a2$) and ($b2$).

4. Application of the Finite-Element Method. The plate is split into Lagrangian finite elements (quadrangular, nine-node, and isoparametric) [8], as is shown, for example, at the right of Fig. 1. In approaching the hole edge and the extreme point of the contact region $\eta = l$, which is regarded as a boundary node between the elements, the elements become smaller. In each mesh, there are 90 finite elements and about 730 unknown variables (displacement components of the nodes of the elements).

Based on the principle of minimum strain energy (1.2), we formulate the finite-element equations for problems (a) and (b). Substituting the corresponding values of displacements at the nodes of the elements on the plate contour into these equations, we obtain the finite-element equations for problems $(a1)$, $(a2)$, $(b1)$, and $(b2)$. To calculate integrals over the element area, the three-point quadrature Gauss formula is used. Each system of finite-element equations is solved using the method of compact Gauss exclusion with allowance for the symmetry and band character of the coefficient matrix, i.e., the global rigidity matrix [8, 9]. The stresses are calculated at the integration points over the element area and interpolated at the nodes of the elements. The small stress discontinuities at the boundaries between the elements in the figures are smoothed.

Below, we give a finite-element solution of the above problems.

5. Solution of Contact Problems. Let us first describe the solution of the contact problems with boundary conditions (2.10). Problem (a) has a solution which is linear in v and c:

$$U^{(a)} = vU^{(a1)} + cU^{(a2)}. \tag{5.1}$$

Hereafter U are the global vectors of the desired variables (displacement components of the nodes of the elements), and the superscript in the parentheses corresponds to the problem from which the marked quantity is taken.

The vectors $U^{(a1)}$ and $U^{(a2)}$ are not dependent on v and c and are found from the solution of the systems of finite element equations of problems $(a1)$ and $(a2)$ which have the same coefficient matrix, namely, the global rigidity matrix. It is calculated and reduced to the triangular form only once for both systems.

At the point $\eta = l$ for σ_{rrl}, which are the limiting values for the radial stresses σ_{rr} on Γ from the side of $\eta < l$, from (5.1) it follows that $\sigma_{rrl}^{(a)} = v\sigma_{rrl}^{(a1)} + c\sigma_{rrl}^{(a2)}$. According to the Boussinesq principle [5, 6], we assume that $\sigma_{rrl}^{(a)} = 0$. Define a displacement $v = v^{(a)}$ that realizes the given contact region:

$$v^{(a)} = -c\sigma_{rrl}^{(a2)}/\sigma_{rrl}^{(a1)}. \tag{5.2}$$

On the basis of the calculation results, we assume that $\sigma_{rrl}^{(a2)} > 0$. Solving problems $(a1)$ for various l by iterations, l of which are similar to those in [3], we obtain a value of $l = l_*^{(a)}$ such that $\sigma_{rrl}^{(a1)} = 0$. If $l < l_*^{(a)}$, then $\sigma_{rrl}^{(a1)} < 0$ and if $l > l_*^{(a)}$, then $\sigma_{rrl}^{(a1)} > 0$. By virtue of (5.2) and the aforesaid, $v^{(a)} < 0$ when $l > l_*^{(a)}$. Therefore, the contact-region length l cannot exceed $l_*^{(a)}$ and approaches $l_*^{(a)}$ as $v = v^{(a)}$ increases infinitely. The maximum length $l_*^{(a)}$ remains the same for any c.

For $c = 0$, $l = l_*^{(a)}$, and arbitrary v, the solution of contact problem (1.1), (2.1), and (2.11) obtained from (5.1) is $U^{(0)} = vU^{(a1)}$. The contact-region length $l_*^{(a)}$ in this problem is not dependent on v.

Substituting $v = v^{(a)}$ with nonzero c from (5.2) into (5.1), we obtain $U^{(a)}$ as a solution of contact problem (1.1), (2.1), and (2.10). It is linear with c. The restrictions in the form of inequalities in (2.10) are satisfied. The vector $U^{(a)}$ as $v = v^{(a)} \to \infty$ and $l \to l_*^{(a)}$ approaches a linear function of v of the form of $vU^{(a1)}$ and almost coincides with $U^{(0)}$ at sufficiently great v.

Let us turn to the case of boundary conditions (2.8). A solution of problem (b) is sought in the form

$$U^{(b)} = vU^{(b1)} + cU^{(b2)}, \tag{5.3}$$

where the vectors $U^{(b1)}$ and $U^{(b2)}$ depend on ε but are not dependent on v. They are calculated by solving the systems of finite-element equations of problems $(b1)$ and $(b2)$ which have the same coefficient matrix, namely the global rigidity matrix, which is ε-dependent. With each new value of ε, in contrast to the case with boundary conditions (2.10), problems $(b1)$ and $(b2)$ and the contact problem as a whole are solved anew.

At the point $\eta = l$, for $q_{\rho l}$ (the limiting values of the normal forces q_ρ on Γ from the side of $\eta < l$),

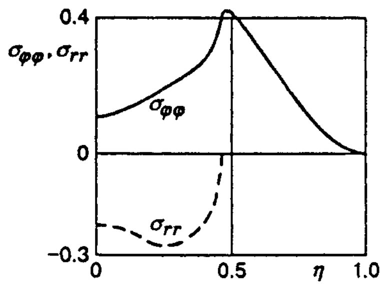

Fig. 2

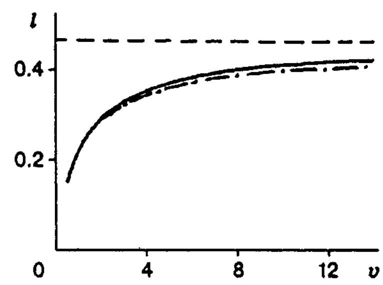

Fig. 3

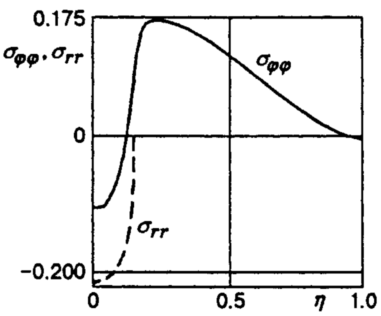

Fig. 4

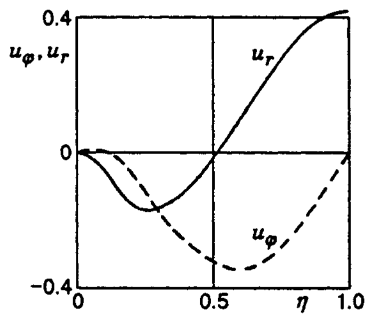

Fig. 5

from (5.3) it follows that $q_{pl}^{(b)} = vq_{pl}^{(b1)} + cq_{pl}^{(b2)}$. On the basis of the Boussinesq principle satisfying the equality $q_{pl}^{(b)} = 0$, we determine a displacement $v = v^{(b)}$ that realizes the given contact region:

$$v^{(b)} = -cq_{pl}^{(b2)}/q_{pl}^{(b1)}. \tag{5.4}$$

Then, by analogy with the previous solution (5.1) and (5.2), on the basis of the calculation results, we assume that $q_{pl}^{(b2)} > 0$. Solving problems ($b1$) for various l, by iterations we find a value of l, $l = l_*^{(b)}$, at which $q_{pl}^{(b1)} = 0$. If $l < l_*^{(b)}$, then $q_{pl}^{(b1)} < 0$, while if $l > l_*^{(b)}$, then $q_{pl}^{(b1)} > 0$. For $v^{(b)}$ to be nonnegative, it is required that $l < l_*^{(b)}$. We have $l \to l_*^{(b)}$ as $v = v^{(b)}$ grows unlimitedly. The maximum length of $l_*^{(b)}$ depends on ε.

Substituting $v = v^{(b)}$ from (5.4) into (5.3), we obtain $U^{(b)}$, which is a solution of contact problem (1.1), (2.1), and (2.8). The restrictions in the form of inequalities in (2.8) are satisfied. As $v = v^{(b)} \to \infty$ and $l \to l_*^{(b)}$, the vector $U^{(b)}$ approaches a linear function of v of the form $vU^{(b1)}$ which depends on ε.

As ε decreases, with the same fixed value of l, problems ($b1$) and ($b2$) approach problems ($a1$) and ($a2$), and the differences between $U^{(b1)}$, $U^{(b2)}$, $v^{(b)}$, and $U^{(b)}$ and, hence, $U^{(a1)}$, $U^{(a2)}$, $v^{(a)}$, and $U^{(a)}$ tend to zero. Moreover, $l_*^{(b)} \to l_*^{(a)}$ as $\varepsilon \to 0$.

6. Analysis of Calculation Results. Let us pass over to nondimensional quantities. For this purpose, we multiply R, L_1, L_2, H, x_1, and x_2 by the nondimensionalizing multiplier R^{-1}, the displacement and the gap c by L_0^{-1}, the strains by $\omega = RL_0^{-1}$, the stresses by ωE^{-1}, and the strain energy Φ by $E^{-1}L_0^{-2}$ (L_0 is a constant with the dimension of length). For nondimensional quantities, we retain the previous notation, and now $R = 1$, $H = L_1 = 2.5$, $L_2 = 5$, and $c = \omega\varepsilon$. The Poisson's ratio is $\nu = 0.3$.

Let us consider the solution $U^{(a1)}$ of contact problem (1.1), (2.1), and (2.11) in the case without a gap for $v = 1$ and $l = l_*^{(a)} = 0.462769$ (which corresponds to the angle πl equal to 83.3°). Separation of the plate into finite elements and its deformed state are shown in Fig. 1. The Cartesian coordinates of the nodes X_i in a deformed state (at the right of Fig. 1) are determined from the initial values of x_i and displacements u_i

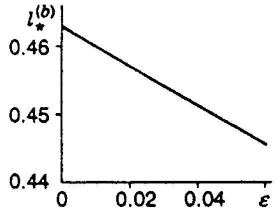

Fig. 6

TABLE 1

Problem	l	P	Φ	$\sigma_{\varphi\varphi(\max)}$	Δ
(0)	0.462769	0.3112	0.2085	0.5620	0.0003436
(a)	0.25	0.2502	0.1563	0.5296	0.0006551
(b)	0.242728	0.2476	0.1548	0.5168	0.0001671

using the formulas $X_i = x_i + \gamma u_i$ $(i = 1, 2)$ (for brevity, hereafter the index of a problem is omitted from the notation of the quantities obtained from its solution). The multiplier $\gamma > 0$ is the same for all u_i and is such that the maximum absolute value of the components of the vector $\gamma\ U^{(a1)}$ equals 1. Transition to the dimensionless quantities of displacements and their multiplication by γ leads to exaggerated strains of the plate. It should also be noted that, in view of linearization of the problem, the section of the hole edge presented as a plate-pin contact region does not lay directly on the pin contour.

The stresses on the hole contour as a function of η are plotted in Fig. 2. The hoop stress $\sigma_{\varphi\varphi}$ is tensile, and the distribution of the radial stress σ_{rr} is nonsinusoidal, with $\sigma_{rr} = 0$ for $l \leqslant \eta \leqslant 1$. The minimum $\sigma_{rr} = -0.2686$ is attained at the internal point of the contact region, while the maximum $\sigma_{\varphi\varphi} = \sigma^*_{\varphi\varphi} = 0.4189$ is attained on the free part of Γ near the point $\eta = l$. The coefficient of stress concentration is $k = HP^{-1}\sigma^*_{\varphi\varphi} = 4.514$. The tensile force

$$P = \int_0^H \sigma_{11} dx_2 \quad \text{for} \quad x_1 = L_2,$$

which is calculated using the quadrature parabola formula [10], is equal to 0.232.

The solution $U^{(a)}$ of contact problem (1.1), (2.1), (2.10) is obtained for $l = 0.15$, 0.2, 0.25, 0.3, 0.35, 0.4, 0.425, and 0.45 and $c = \omega\varepsilon = 1$. It is applicable for any not too large gap given by ε. As v grows, the solid curve of l in Fig. 3 vs. $v = v^{(a)}$ approaches the dashed curve on which $l = l_*^{(a)}$.

On the whole, the stress distribution in the plate for $l > 0.25$ is similar to that given above in the solution of $U^{(a1)}$ for the case without a gap; only the position of the point $\eta = l$ changes. With $l \leqslant 0.25$, in the vicinity of the point $(-R, 0)$ at the hole edge and near it there is a small region in which $\sigma_{r\varphi}$ is small in absolute value, and $\sigma_{rr} < 0$ and $\sigma_{\varphi\varphi} < 0$.

Figures 4 and 5 show the distribution of the stresses σ_{rr} and $\sigma_{\varphi\varphi}$ and the displacements u_r and u_φ on Γ for $l = 0.15$ and $v = v^{(a)} = 0.4993$. The minimum σ_{rr} is at the point $\eta = 0$. In most of the contact region, $\sigma_{rr} < 0$, $\sigma_{\varphi\varphi} < 0$ and $u_\varphi > 0$. As l and v increase, the section on Γ with positive hoop displacements disappears.

Let us now compare $U^{(a)}$ with the solution $U^{(b)}$ of problem (1.1), (2.1), and (2.8). As ε increases, the maximum length of the contact region $l_*^{(b)}$ decreases almost linearly with respect to ε (Fig. 6). The decrease in $l_*^{(b)}$ is small compared with $l_*^{(a)}$ and for $\varepsilon = 0.05$, it is about 3%.

The relative values of the differences between $U^{(a)}$ and $U^{(b)}$ are of the same order of smallness for $\varepsilon = 0.05$ and equal displacements $v = v^{(a)} = v^{(b)}$. The above characteristic properties of $U^{(a)}$ are also retained by $U^{(b)}$. The dependence of l on $v = v^{(b)}$ is presented in Fig. 3 by a dot-and-dashed curve for $l_*^{(b)} = 0.448351$.

In comparison with (2.10), the variant of boundary conditions (2.8) is less restrictive for the plate. With the same displacement v, it gives rise to smaller values of the strain energy, maximum stresses, contact-region length, and force P. The distance from the deformed edge of the hole to the pin contour is determined in dimensionless quantities by the formula

$$\Delta = [(1 + \varepsilon \cos\varphi + \omega^{-1}u_r)^2 + (-\varepsilon \sin\varphi + \omega^{-1}u_\varphi)^2]^{1/2} - (1 - \varepsilon).$$

In the problems considered, on the contact section Δ is not strictly equal to zero, but it is smaller in problem (b) than in problem (a). Table 1 presents the values of Δ at the points $\eta = l$, the maximum values of hoop stresses $\sigma_{\varphi\varphi}$ on Γ denoted by $\sigma_{\varphi\varphi(\max)}$, the values of l, P, and Φ in the solutions $U^{(a)}$ and $U^{(b)}$ for $\varepsilon = 0.05$, and also in the solution $U^{(0)} = vU^{(a1)}$ [problem (0) in Table 1], with $v = v^{(a)} = v^{(b)} = 1.341$.

Having compared $U^{(a)}$, $U^{(b)}$, and $U^{(0)}$ under equal displacements v, we note the following. As l grows, the difference in $U^{(a)}$ and $U^{(b)}$ can become arbitrarily large because of the unbounded growth of $U^{(a)}$ and $U^{(b)}$ and different $l_*^{(a)}$ and $l_*^{(b)}$.

REFERENCES

1. M. W. Hyer and E. C. Klang, "Contact stresses in pin-loaded orthotropic plates," *Int. J. Solids Struct.*, **21**, No. 9, 957–975 (1985).
2. R. A. Naik and J. H. Crews (Jr.), "Stress analysis method for a clearance-fit bolt under bearing loads," *AIAA J.*, **24**, No. 8, 1348–1353 (1986).
3. V. N. Solodovnikov, "Stresses in a plate kept in equilibrium by a pin," *Prikl. Mekh. Tekh. Fiz.*, No. 1, 144–147 (1990).
4. P. D. Mangalgiri, B. Dattaguru, and A. K. Rao, "Finite element analysis of moving contact in mechanically fastened joints," *Nucl. Eng. Des.*, **78**, 303–311 (1984).
5. J. Boussinesq, *Application des Potentials à l'Étude de l'Équilibre et du Mouvement des Solides Élastiques*, Gauthier-Villard, Paris (1885).
6. K. L. Johnson, *Contact Mechanics*, Cambridge Univ. Press, England (1985).
7. S. P. Timoshenko and J. Gudier, *Theory of Elasticity*, McGraw-Hill, New York (1970).
8. K. J. Bathe, *Finite Element Procedures in Engineering Analysis*, Prentice-Hall, Englewood Cliffs, New Jersey (1982).
9. D. K. Fadeev and V. N. Fadeeva, *Computational Methods in Linear Algebra* [in Russian], Fizmatgiz, Moscow–Leningrad (1963).
10. V. I. Krylov, *Approximate Calculation of Integrals* [in Russian], Fizmatgiz, Moscow (1959).